A major purpose of the Technical Information Center is to provide the broadest dissemination possible of information contained in DOE's Research and Development Reports to business, industry, the academic community, and federal, state and local governments.

Although a small portion of this report is not reproducible, it is being made available to expedite the availability of information on the research discussed herein.

LA-UR--84-3440

DE85 002433

CONF-850103--3

TITLE SPACE NUCLEAR-POWER REACTOR DESIGN BASED ON COMBINED NEUTRONIC AND THERMAL-FLUID ANALYSES

AUTHOR(S) D. R. Koenig, C-6
R. G. Gido, Q-7
D. I. Brandon, Q-12

SUBMITTED TO Space Nuclear Power Systems Symposium, Albuquerque, NM, January 8-13, 1985

Los Alamos National Laboratory
Los Alamos, New Mexico 87545

SPACE NUCLEAR-POWER REACTOR DESIGN
BASED ON COMBINED NEUTRONIC AND THERMAL-FLUID ANALYSES

D.R. Koenig, R.G. Gido and D.I. Brandon

Los Alamos National Laboratory

MS-K988,* P.O. Box 1663

Los Alamos, NM 87545

Phone:* 505-667-7035 FTS 843-7035

ABSTRACT

The design and performance analysis of a space nuclear-power system requires sophisticated analytical capabilities such as those developed during the nuclear rocket propulsion (Rover) program. In particular, optimizing the size of a space nuclear reactor for a given power level requires satisfying the conflicting requirements of nuclear criticality and heat removal. The optimization involves the determination of the coolant void (volume) fraction for which the reactor diameter is a minimum and temperature and structural limits are satisfied. A minimum exists because the critical diameter increases with increasing void fraction, whereas the reactor diameter needed to remove a specified power decreases with void fraction. The purpose of this presentation is to describe and demonstrate our analytical capability for the determination

*Mail stop and phone are for D.R. Koenig.

of minimum reactor size. The analysis is based on combining neutronic criticality calculations with OPTION-code thermal-fluid calculations.

INTRODUCTION

There is considerable interest currently in a wide variety of large space power sources ranging from a few megawatts of steady-state electric power (MW_e) to 100 MW_e of pulsed power. This power range is clearly beyond the capabilities of solar power sources and it lies eminently in the domain of nuclear power, with some competition from chemical sources for short mission durations. Until definite mission requirements emerge, it is unclear at this stage whether we should develop open- or closed-cycle power plants, dual-mode nuclear power plants capable of generating moderate amounts of steady-state power plus high pulsed power, or dual-mode hybrid systems where steady-state power would be generated by a small nuclear reactor and large pulsed power by a chemical power source.

The legacy of the nuclear rocket engines developed during the Rover program in the sixties and early seventies provides a relevant technology base that we can draw on to help us in our scoping and design studies, Koenig (1984), Buden (1984). Some 20 different reactor tests were conducted in this period ranging in power from 50 to 4000 thermal megawatts (MW_t). Major accomplishments of the Rover program are shown in Fig. 1. Indeed many of these demonstrated accomplishments of temperature, duration at power, power density, and restarting capability exceed requirements that will be imposed on the space nuclear reactors of current interest. The Rover reactors were hydrogen-gas-cooled epithermal reactors fueled with UC in a graphite matrix. The radial reflector was beryllium containing rotating drums with segments of B_4C neutron poison for

reactivity control. A typical reactor is described in Fig. 2. What makes this reactor design particularly interesting beyond its demonstrated capability is that it can be adapted to either open- or closed-loop power plants, and furthermore, it can be modified for dual-mode operation, Beveridge (1971), Altseimer (1973).

This latter capability is made possible because the tie-tube support elements in the reactor core are cooled by a separate circuit from the main coolant flow and this circuit could readily be converted into a closed-cycle power plant for steady-state, small power generation, as shown in Figs. 3 and 4.

For the initial exploratory studies described in this paper we have chosen to model the last reactor design studied under the Rover program by the Los Alamos National Laboratory, the so-called Small Engine reactor design, Durham (1972), Balcomb (1972). This reactor, which was never built, represents the culmination of what was learned during project Rover, and at a design power level of 367 MW_t, it lies within the power range of interest today. Using thermal-hydraulic and neutronic analysis tools and an optimization methodology discussed in this paper we have made a preliminary assessment of the mass and size of this reactor design as a function of power level when used as the power source for an open-cycle power plant.

SMALL-ENGINE REACTOR DESIGN

A flow diagram for the Small Engine is shown in Fig. 5. The engine uses hydrogen as the propellant. It employs a full-flow topping cycle whereby the entire propellant flow eventually passes through the hot core. It has regeneratively cooled nozzle and tie-tube support elements. The coolant flow through the tie tubes drives a single-stage centrifugal pump with a single-stage

turbine. The engine requires only five valves for operation. For power generation the nozzle would be replaced by a turbo alternator and the hydrogen gas exhausted in such a way as not to produce thrust. The mass of the entire Small Engine is 2500 kg.

The reactor core, pictured in Fig. 6, was designed to produce 367 MW_t within a diameter of 57 cm and a height of 89 cm. It consists of 564 hexagonally shaped fuel elements, each having 19 coolant channels. In addition, the core has 241 support elements containing zirconium hydride, ZrH_2, as a neutron moderator. This moderating material reduces the critical size of the reactor, which contains only 36 kg of fully enriched ^{235}U. More details on the fuel modules are shown in Fig. 7. The fuel provides the energy and the heat-transfer surface for heating the hydrogen. It consists of 93.15% ^{235}U in a composite matrix of UC-ZrC solid solution and carbon. The channels are coated with zirconium carbide to protect against hydrogen reactions. The tie tubes serve three functions: transmitting the core axial pressure load from the hot end of the fuel elements to the core-support plate at the core inlet; providing an energy source for the turbo pump; and containing and cooling the zirconium hydride moderator sleeves by a counter-flow arrangement. The core is surrounded by a thermal insulator and slats that encircle the periphery. The beryllium radial reflector contains 12 rotating reactivity control drums. The core is supported at the cold-inlet end by an aluminum alloy support plate that rests on the reflector assembly, and the entire reactor is contained within an aluminum pressure vessel. The reactor was designed for 83 K/s thermal transients.

ANALYSIS

In this section our thermal-fluid and neutronic analytical capabilities are described and applied to the design of a space power reactor like the Rover Small Engine.

Thermal-Fluid Analysis

The design and performance analysis of a space nuclear-power system requires sophisticated thermal-fluid analytical capability. For example, optimizing the size of a space nuclear reactor for a given power level involves determination of the diameter vs coolant void fraction relationship that satisfies temperature (because of corrosion) and temperature-difference (because of thermal-stress) limits. The purpose of this section is to describe and demonstrate our thermal-fluid analytical capability based on the OPTION code, McClary (1968).

OPTION was developed and used extensively for the design, pretest and posttest analyses of the Rover-program 100-1000 MW gas-cooled nuclear-rocket reactor systems that were built and tested from 1960 to 1970. The analyses included determination of the core geometry, core orificing to balance flow, and reflector and periphery cooling design. The code capability descriptions, procedures for code use and results of code analyses are well documented, McFarland (1969), Sibbitt (1969), House (1970), Merson (1972).

Generality in OPTION modeling capability is achieved by provision for a library of optional (hence the code name) subprograms. The optional capability provides for most facets of a thermal-fluid analysis, including

1. specification of flow branching and mixing network,
2. problem boundary-condition specifications, which can be based on any

combination of fluid temperatures and pressures, flow rates and power generation,

3. flow-passage geometries and configurations,
4. solid-component geometries,
5. internal heat generation,
6. fluid and solid properties,
7. convective heat-transfer and friction-factor correlations, and
8. output formatting.

As a result, the user can select from existing options or add options for the problem of interest. For example, the flow equation available is for a compressible gas with a velocity less than the speed of sound. However, another flow equation option, such as that for a liquid metal or a heat pipe, could be added. At this time, the code is for steady-state analysis.

Figure 8 depicts the Small Engine reactor core-cluster model corresponding to the fuel module in Fig. 7, analyzed using OPTION. This model demonstrates the code capability to solve problems involving

1. parallel and counterflow,
2. transverse thermal communication (axial conduction is ignored) between the flow passages and peripheral boundaries, and
3. solids with internal power generation and potentially complex geometries.

The finite-element mesh developed specifically for this problem is shown in Fig. 9. As a result, a detailed accounting of the conduction heat transfer and temperature distribution for stress analysis are provided. Note that the cluster geometric specification was made arbitrary so that design optimization studies could be made.

A flow diagram for the OPTION model described by Figs. 8 and 9 is given in Fig. 10, which also shows the transverse heat transfer between flow channels. Figure 11 is an OPTION flow diagram for the complete space power system described in Fig. 5. Note that the model includes the supply tank, pump, turbine, valves, tie tubes, nozzle, reflector and the reactor fuel elements. An OPTION model such as this could be used to analyze the operation of a dual-mode space-power system, such as discussed in the introduction.

To demonstrate the capability of the OPTION code, preliminary calculations were performed to determine the Small Engine reactor-core diameter vs coolant void fraction for different power levels as shown in Fig. 12. The calculation were based on a simple, single-channel flow model of the core, using the following assumptions:

1. Inlet temperature of 370 K (666 R).
2. Exit temperature of 1500 K (2700 R).
3. Exit pressure of 3.10 MPa (450 psia).
4. Exit Mach number of 0.25.
5. Axial power density profile shown in Fig. 13.

Other code results that are important include fuel and fluid temperature profiles shown in Fig. 14 and the pressure drop.

The results presented in Fig. 14 could be used to impose constraints, such as corrosion (temperature) and thermal stress (temperature difference) limits. Other constraints that might be imposed include manufacturability (web thickness) and structural limitations (e.g., pressure drop). Note that the results presented in Fig. 12 do not reflect the imposition of these constraints because the OPTION calculated temperature level, temperature differences and pressure drops were approximately within acceptable limits.

Neutronic Criticality Analysis

The thermal analysis results shown in Fig. 12 describe how, for specified power levels, core size varies as a function of coolant void fraction. And obviously, as coolant void fraction increases it becomes easier to extract power from the core and core size decreases. These curves, however, tell us nothing about where on the curves the reactor achieves neutronic criticality. And what is needed to find the optimum reactor design is a similar plot of critical core diameter vs void fraction. The Small-Engine reactor has an epithermal neutron energy spectrum and a heterogeneous core configuration because of the zirconium-hydride moderating material in the core support element.

For these reasons we have chosen to analyze this reactor with the Monte Carlo Neutron and Photon (MCNP) transport code, Los Alamos Monte Carlo Group (1981). The MCNP code has the capability of modeling complex, three-dimensional geometries as shown in the 30° sector of the Small Engine reactor in Fig. 15, where every core support element and reflector control drum have been included. In addition, the MCNP code employs continuous-energy neutron cross-sections. These two features avoid the uncertainties associated with homogenizing the core and the reflector and generating effective, multigroup, resonance self-shielded, properly diluted cross sections, as one is forced to do with traditional discrete-ordinate transport codes. The MCNP calculation also permits an accurate determination of the reactivity swing available from the reflector control system. The available control margin is an important design parameter for large power generation because reactivity loss caused by burnup of fuel and the corresponding poisoning from fission products can place severe limitations on the system life.

The Small-Engine reactor model shown in Fig. 15 was scaled to other sizes by adding or subtracting support elements and corresponding fuel. This is accomplished through the use of a preprocessor code that permits easy modification of the reference reactor (Small-Engine design). Other modifications that can readily be incorporated include varying the relative dimensions of the support and fuel elements and varying the amount of moderating material in the support elements. The fuel loading in each core zone is adjusted to maintain a flat radial power profile. For the present work the thickness of the reflector assembly and the number of control drums were kept constant. Results of critical core diameter vs coolant channel void fraction are displayed in Fig. 16 for several choices of core length. We have chosen to define critical configuration as that corresponding to a multiplication factor $k_{eff} = 1.05$ with the control drum in the most reactive position.

As expected, for a fixed core length the critical core diameter increases as void fraction increases because the core average fuel density decreases tending to make the reactor less critical. Also included in Fig. 16 for comparison are the thermal-fluid analysis results of Fig. 13. These latter curves are not functions of core length.

Reactor Mass Analysis

The intersection between one of the criticality curves in Fig. 16 and one of the heat removal (flow rate) curves gives the minimum core diameter and the corresponding channel void fraction for which both heat removal and critical size requirements are met. At a smaller diameter there is not enough channel space to extract the desired power from the core and not enough fuel to achieve a critical configuration. The mass of the reactor can be computed at the

intersection points and plotted vs core length as shown in Fig. 17 where it seems that for the range of power levels chosen, minimum reactor mass occurs at a core length of 0.8-0.9 m. A plot of minimum reactor mass as a function of power level is shown in Fig. 18. A system code is currently being written to automate this optimization process.

The significance of the results presented in Fig. 18 is that this curve represents the mass/power functional dependence of the Small-Engine reactor design scaled to various power levels for the coolant core inlet and outlet conditions specified in the Thermal-Fluid Analysis section. These conditions are representative of what could be expected for an advanced, hydrogen gas, open-cycle, Brayton power plant. However, a different choice of conditions would lead to a different reactor mass vs power curve. The results shown in Fig. 18 are not definitive in terms of what can be achieved with gas-cooled reactors of the Rover type. Rather, they have been included to demonstrate the capabilities of our design tools. According to Fig. 18, the mass of the Small-Engine reactor design for the chosen operating conditions is comparable to that of the particle bed reactor, Powell (1983).

CONCLUSIONS AND RECOMMENDATIONS

We offer the following conclusions and recommendations:

1. The demonstrated technology of the Rover nuclear rocket program should be used as a basis for the development of high-power nuclear reactors for electric power generation in space.
2. The reactor designs developed and tested during the Rover program could be applied with minor modifications as energy sources for space nuclear power plants.

3. The Small Engine reactor, designed late in the Rover program could be used to illustrate the relevance of the Rover technology to space power generation.
4. The demonstrated technology of the Rover program lies not only in reactor designs, but also in analysis tools that were originally developed during that period, tools such as the versatile thermal-fluid analysis code OPTION and the Monte Carlo neutron and photon transport code MCNP.
5. Methodologies using Rover-developed codes to optimize reactor designs can be applied to calculate the functional dependence of mass and power for space nuclear power plants.
6. We have applied this methodology for one set of open-cycle coolant conditions of the Small-Engine reactor design.
7. The mass of an optimized reactor based on these procedures is indeed quite light, being approximately 2000 kg at a power of 200 MW_t.
8. The OPTION thermal-fluid code optional capabilities should be expanded to include models for components (e.g. valves, turbines, and pumps) and physical processes (e.g., heat pipes) required for the analysis of complete space nuclear power reactors.

ACKNOWLEDGEMENTS

This work was supported by the Air Force Weapons Laboratory, Kirtland Air Force Base, Kirtland, NM, and coordinated by Col. Jim Lee.

REFERENCES

Altseimer, J.H., and L.A. Booth (1972) "Nuclear Rocket Energy Center Concept," Los Alamos National Laboratory Report LA-DC-72-1262.

Balcomb, J.D. (1972) "Nuclear Rocket Reference Data Summary," Los Alamos National Laboratory Report LA-5057-MS.

Beveridge, J.H. (1971) "Feasibility of Using the NERVA Rocket Engine for Electrical Power Generation," AIAA paper No. 71-639, AIAA/SAE 7th Propulsion Joint Specialist Conference, Salt Lake City, Utah, June 14-18.

Buden, D. and J.A. Angelo (1984), "Space Nuclear Power" (in publication).

Durham, F.P. (1972) "Nuclear Engine Definition Study Preliminary Report," Los Alamos National Laboratory Report LA-5044-MS, Vol. I-III.

House, L. (1970) "Arbitrary Geometry Conduction Solution for OPTION-2," Los Alamos Scientific Laboratory internal memo N-7-842 (Sept. 9).

Koenig, D.R. (1984), "Experience Gained from the Space Nuclear Rocket Program (Rover)," Los Alamos National Laboratory Report LA-10062-H (in publication)

McClary, J.A., S.T. (Murray) Smith, and R.G. Gido (1968) "OPTION - A Computer Code to Solve Steady-State Fluid-Thermal Engineering Problems," Los Alamos Scientific Laboratory internal memo N-7-544.

McFarland, R.D. (1969) "PEWEE 1 Fuel/Center Element Flow Bypass," Los Alamos Scientific Laboratory internal memo N-7-667 (May 12).

Merson, T.J. (1972) "Fuel Channel Parameter Study for the Flight Reactor," Los Alamos Scientific Laboratory internal memo N-3-2076 (Apr. 12).

Powell, J.R., and T.E. Botts (1983) "The FBR and RBR Particle Bed Space Reactors," Proc. 18th Intersociety Energy Conversion Engineering Conference, Orlando, Florida, p. 1200, Aug. 21-26.

Sibbitt, W.L. (1969) "Thermal Conductivity of Fuel and Support Elements in PEWEE 2," Los Alamos Scientific Laboratory internal memo N-7-732 (Nov. 6).

CAPTIONS FOR FIGURES

Fig. 1

Major accomplishments of the Rover nuclear rocket program. Note that the temperature and power levels achieved are much higher than those needed for space nuclear power plants.

Fig. 2

Rover reactor design features.

Fig. 3

Dual-mode Rover power plant flow diagram. Note the recirculation loop through the tie-tube supports provides steady-state low power for station keeping.

Fig. 4

Dual-mode nuclear rocket flow diagram showing use of tie-tube support thermal energy for low-power electrical mode.

Fig. 5

Rover Small-Engine flow diagram and general description. Note that the tie-tube coolant is used to operate the turbine that pumps the propellant.

Fig. 6

Rover program Small-Engine reactor core cross section. See Figs. 2 and 5 also.

Fig. 7

Rover program Small-Engine reactor fuel model. See Figs. 2, 5 and 6.

Fig. 8

Gas-cooled space nuclear power system fuel-support element cluster configuration (see Fig. 7) analyzed with the OPTION thermal-fluid code. Analysis based on triangular region of symmetry that is shaded, see Fig. 9.

Fig. 9

Finite-element mesh for the OPTION-code determination of transverse conduction and temperature distribution for the cluster configuration shown in Fig. 7. Note that the model includes representation of the coatings, possible gaps, and a complicated geometry. Geometric specification is arbitrary, i.e., the coolant diameters, coating and gap thickness, hole spacings, etc. are input.

Fig. 10

OPTION flow diagram showing flow channels, flow junctions and transverse heat-transfer paths between channels for cluster configuration shown in Figs. 8 and 9.

Fig. 11

OPTION flow diagram showing flow channels, flow junctions, valves, nozzle, reflector, pump, turbine, and transverse heat-transfer paths between channels for a complete space-power system as depicted in Fig. 5.

Fig. 12

Reactor core diameter (m) vs coolant channel void fraction for several power levels. MW_t is thermal power level and MW_e is electrical power level (conversion efficiency of 0.50). The calculations are for an inlet temperature of 370 K (666 R) and exit conditions of 1500 K (2700 R), 3.10 MPa (450 psia) and Mach number of 0.25.

Fig. 13

Axial power profile used for OPTION thermal-fluid analysis.

Fig. 14

Typical OPTION thermal-fluid code temperature and heat-transfer coefficient vs core length profiles.

Fig. 15

Monte Carlo neutron and photon transport code radial cross section of reactor.

Fig. 16

Thermal-fluid and neutronic analysis results. A mass analysis at the intersections of these results is shown in Fig. 17.

Fig. 17

Core length vs reactor mass for several power levels based on the thermal-fluid and neutronic analytical results given in Fig. 16.

Fig. 18

Power level vs reactor mass corresponding to the minimum core diameters for the curves of Fig. 17.

RECORD PERFORMANCES

POWER (PHOEBUS 2A)	4100 MW
THRUST (PHOEBUS 2A)	~930,000 N
HYDROGEN FLOW RATE (PHOEBUS 2A)	120 kg/s
EQUIVALENT SPECIFIC IMPULSE (PEWEE)	~845 s
MINIMUM REACTOR SPECIFIC MASS (PHOEBUS 2A)	2.3 kg/MW
AVERAGE COOLANT EXIT TEMPERATURE (PEWEE)	2550 K
PEAK FUEL TEMPERATURE (PEWEE)	2750 K
CORE AVERAGE POWER DENSITY (PEWEE)	2340 W/cm^3
PEAK FUEL POWER DENSITY (NF-1)	4500 W/cm^3
ACCUMULATED TIME AT FULL POWER (NF-1)	109 min
GREATEST NUMBER OF RESTARTS (XE)	28

Fig. 1. Major accomplishments of the Rover nuclear rocket program. Note that the temperature and power levels achieved are much higher than those needed for space nuclear power plants.

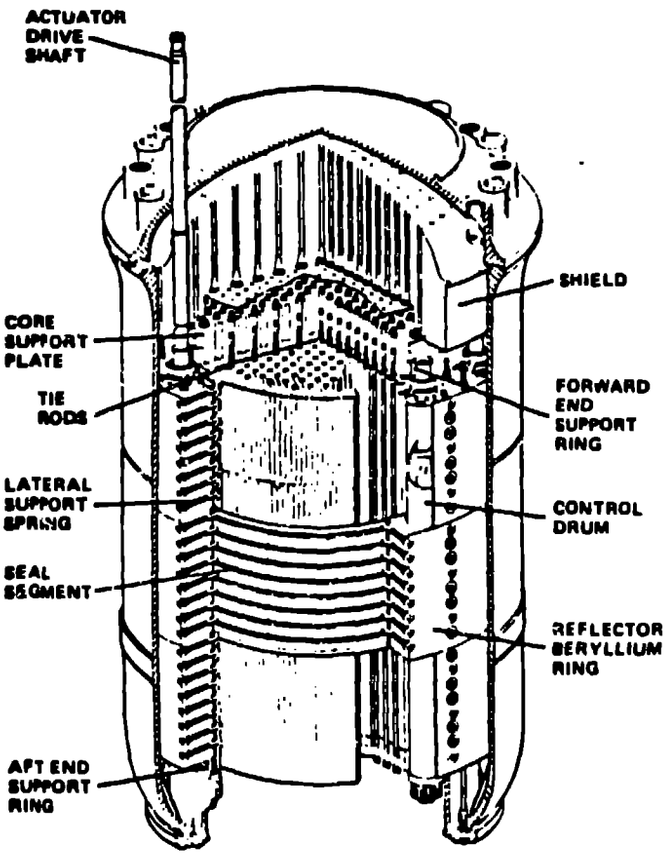

- EPI-THERMAL, GRAPHITE-MODERATED, HYDROGEN-COOLED REACTOR
- USED ENRICHED 93.15% URANIUM-235 AS FUEL
- POWER FLATTENING BY VARYING FUEL LOADING AND FLOW DISTRIBUTION
- CORE INLET ORIFICES CONTROL FLOW DISTRIBUTION
- CORE SUPPORTED BY COLD-END SUPPORT PLATE AND STRUCTURAL TUBE ARRANGEMENT
- REACTIVITY CONTROL BY ROTATING DRUMS IN REFLECTOR CONTAINING NEUTRON ABSORBER

Fig. 2. Rover reactor design features.

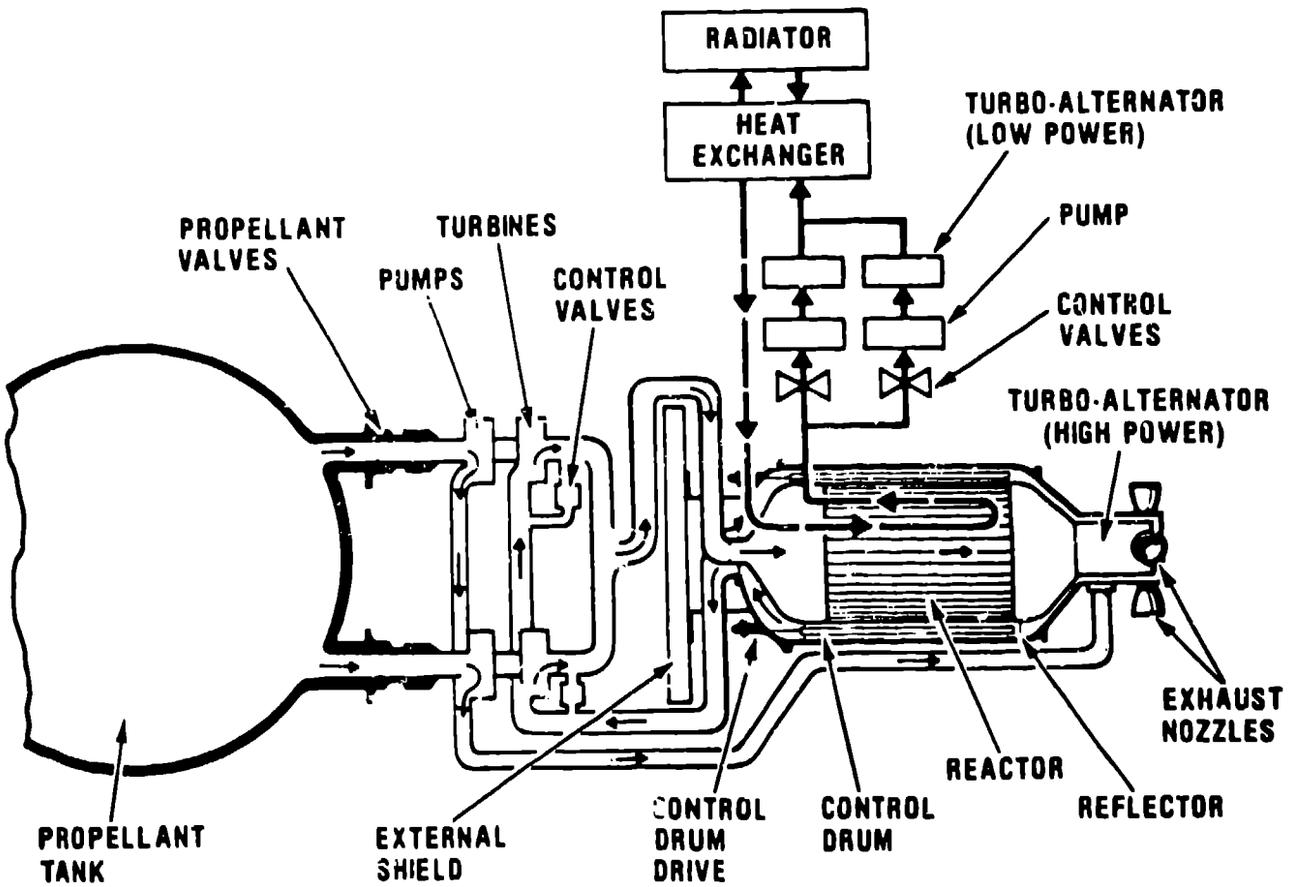

Fig. 3. Dual-mode Rover power plant flow diagram. Note the recirculation loop through the tie -tube supports provides steady-state low power for station keeping.

MODES

- HIGH-POWER ROCKET MODE OF 365 MW, 10 h LIFE, 2600-2660 K PROPELLANT TEMPERATURE, NEGLIGIBLE FUEL BURNUP
- LOW-POWER ELECTRICAL MODE OF 10-25 kW(e), 1 MW(t), ORGANIC RANKINE CYCLE DRIVEN BY THERMAL ENERGY FROM STRUCTURAL SUPPORT SYSTEM, USES PROPULSION MODULE SURFACE TO SUPPORT RADIATOR UP TO 10 kW(e)

ENGINE MODIFICATIONS

- STRUCTURAL SUPPORT SYSTEM ISOLATION VALVES FOR LOW-POWER
- CHANGE REACTOR DOME AND TIE TUBE CORE SUPPORT PLATE LINES FOR WIDER TEMPERATURE RANGE OPERATION TO STAINLESS STEEL FROM Al, AND ACTUATOR WINDINGS TO CERAMIC FROM POLYIMIDE

LIFETIME

- STUDY SHOWED TWO YEARS LIFE WILL NOT SIGNIFICANTLY AFFECT REACTIVITY CONTROL MARGIN

*STUDIED IN EARLY 1970's BY J. ALTSEIMER, L. A. BOOTH, "THE NUCLEAR ROCKET ENERGY CENTER CONCEPT" LA-DC-72-1262, 1973, BASED ON IDEAS OF JOHN BEVERIDGE

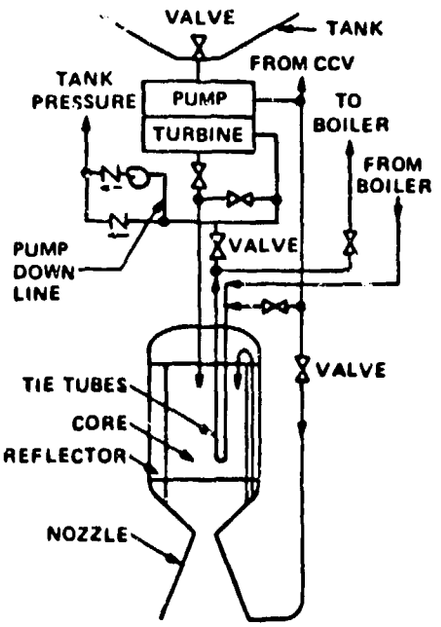

Fig. 4. Dual-mode nuclear rocket flow diagram showing use of tie-tube support thermal energy for low-power electrical mode.

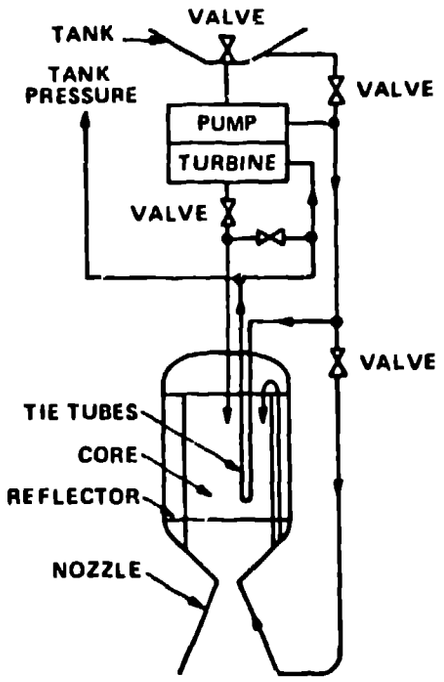

- HYDROGEN PROPELLANT
- FULL FLOW TOPPING CYCLE
- SINGLE-STAGE CENTRIFUGAL PUMP AND SINGLE-STAGE TURBINE
- REGENERATIVELY COOLED METAL-CORE SUPPORT ELEMENTS (TIE TUBES)
- RADIATION SHIELD OF BORATED ZIRCONIUM HYDRIDE
- 6 CONTROL-DRUM ACTUATORS
- 5 VALVES AND VALVE ACTUATORS
- REGENERATIVELY COOLED NOZZLE, AREA RATIO = 25:1
- UNCOOLED NOZZLE SKIRT, EXIT AREA RATIO = 100:1
- UNCOOLED NOZZLE SKIRT HINGED AND ROTATABLE
- OVERALL ENGINE LENGTH =
  - 3.1 m (123 in.) WITH SKIRT FOLDED
  - 4.4 m (174 in.) WITH SKIRT IN PLACE
- TOTAL MASS = 2550 kg (5620 lb)

Fig. 5. Rover Small-Engine flow diagram and general description. Note that the tie-tube coolant is used to operate the turbine that pumps the propellant.

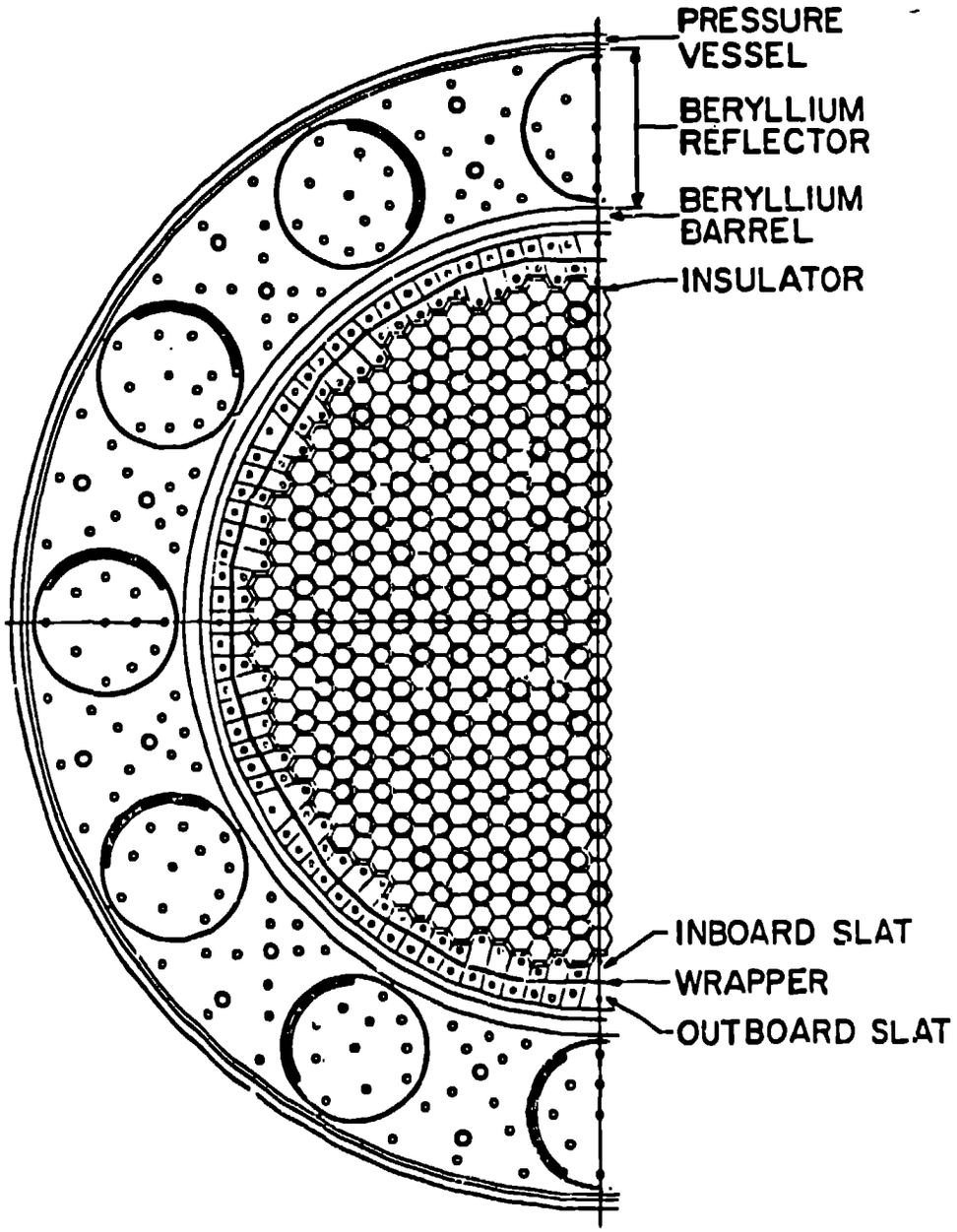

Fig. 6. Rover program Small-Engine reactor core cross section. See Figs. 2 and 5 also.

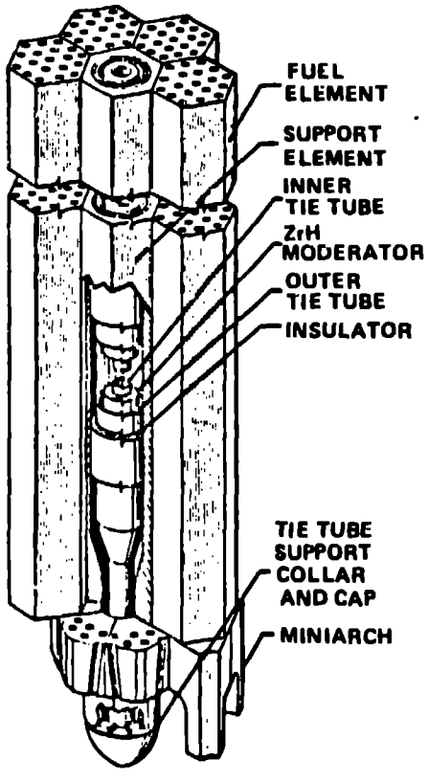

FUEL

- FUNCTION
  - PROVIDED ENERGY FOR HEATING HYDROGEN PROPELLANT
  - PROVIDED HEAT TRANSFER SURFACE
- DESCRIPTION
  - ^{235}U IN A COMPOSITE MATRIX OF UC-ZrC SOLID SOLUTION AND C
  - CHANNELS COATED WITH ZrC TO PROTECT AGAINST H_2 REACTIONS

TIE TUBES

- FUNCTION
  - TRANSMIT CORE AXIAL PRESSURE LOAD FROM THE HOT END OF THE FUEL ELEMENTS TO THE CORE SUPPORT PLATE
  - ENERGY SOURCE FOR TURBOPUMP
  - CONTAIN AND COOL ZrC MODERATOR SLEEVES
- DESCRIPTION
  - COUNTER FLOW HEAT EXCHANGER OF INCONEL 718
  - ZrH MODERATOR
  - ZrC INSULATION SLEEVES

Fig. 7. Rover program Small-Engine reactor fuel model. See figs. 2, 5 and 6.

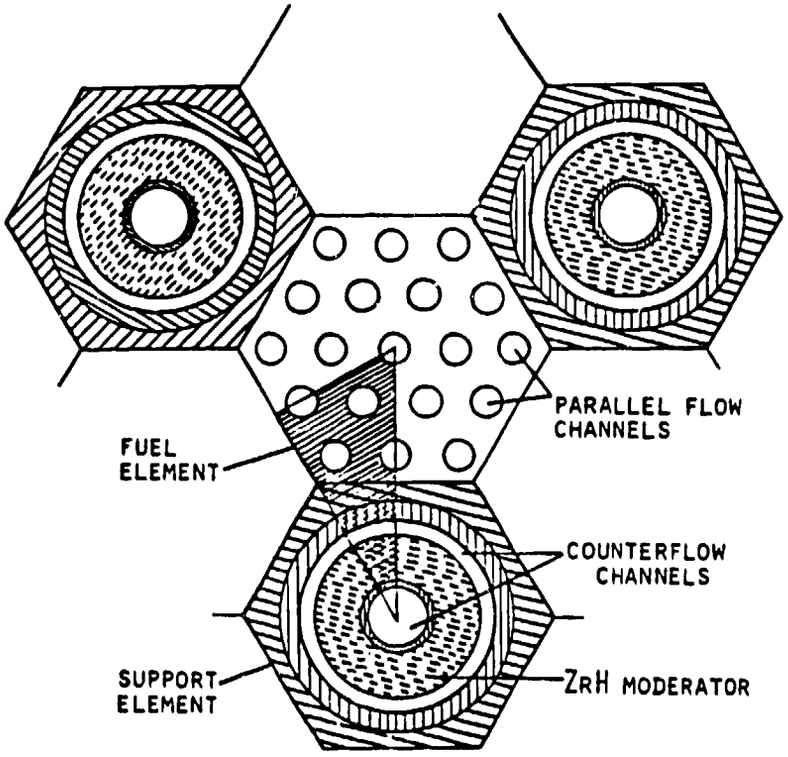

Fig. 8. Gas-cooled space nuclear power system fuel-support element cluster configuration (see Fig. 7) analyzed with the OPTION thermal-fluid code. Analysis based on triangular region of symmetry that is shaded, see Fig. 9.

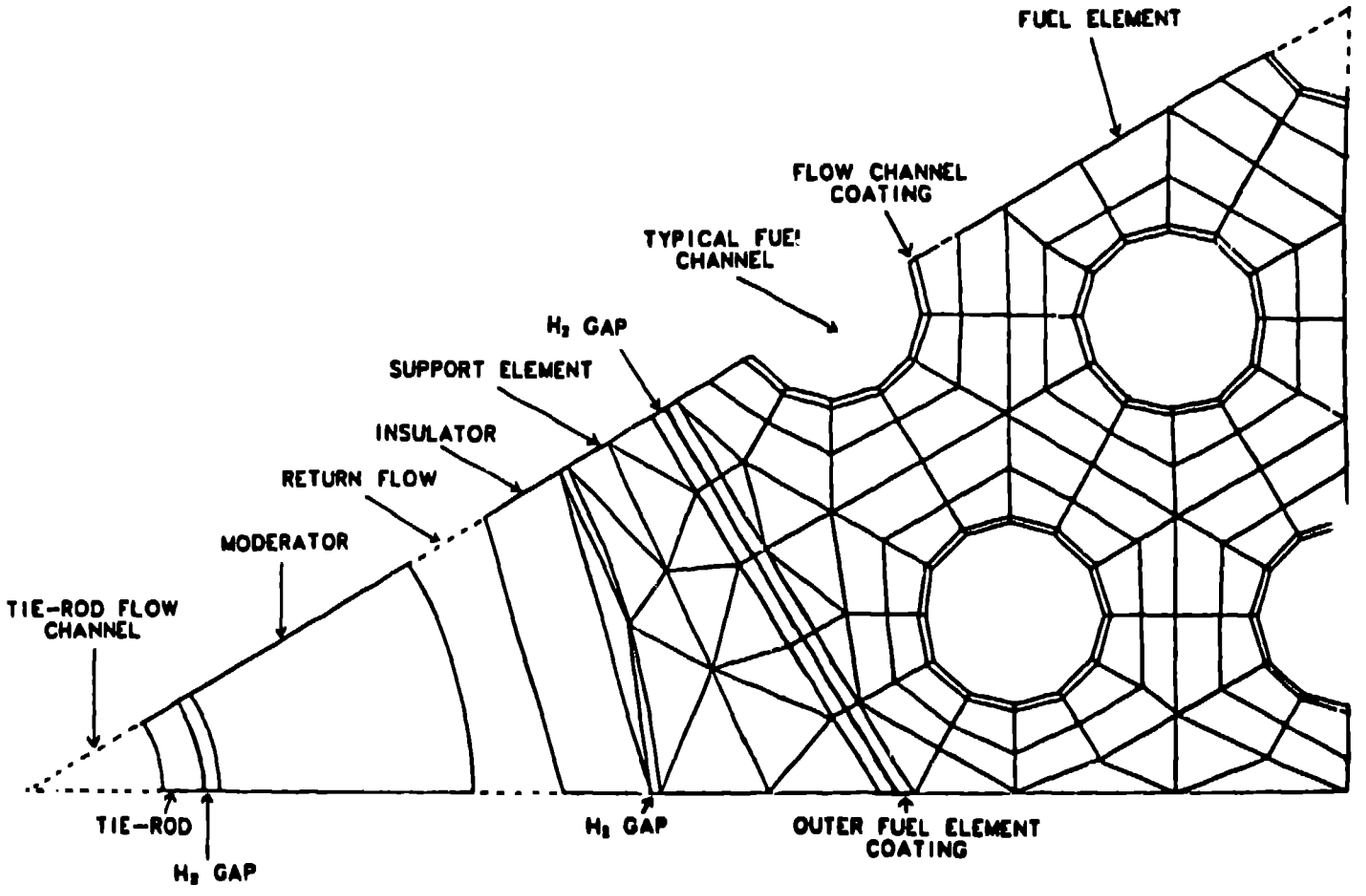

Fig. 9. Finite-element mesh for the OPTION-code determination of transverse conduction and temperature distribution for the cluster configuration shown in Fig. 7. Note that the model includes representation of the coatings, possible gaps, and a complicated geometry. Geometric specification is arbitrary, i.e., the coolant diameters, coatings and gap thickness, hole spacing, etc. are input.

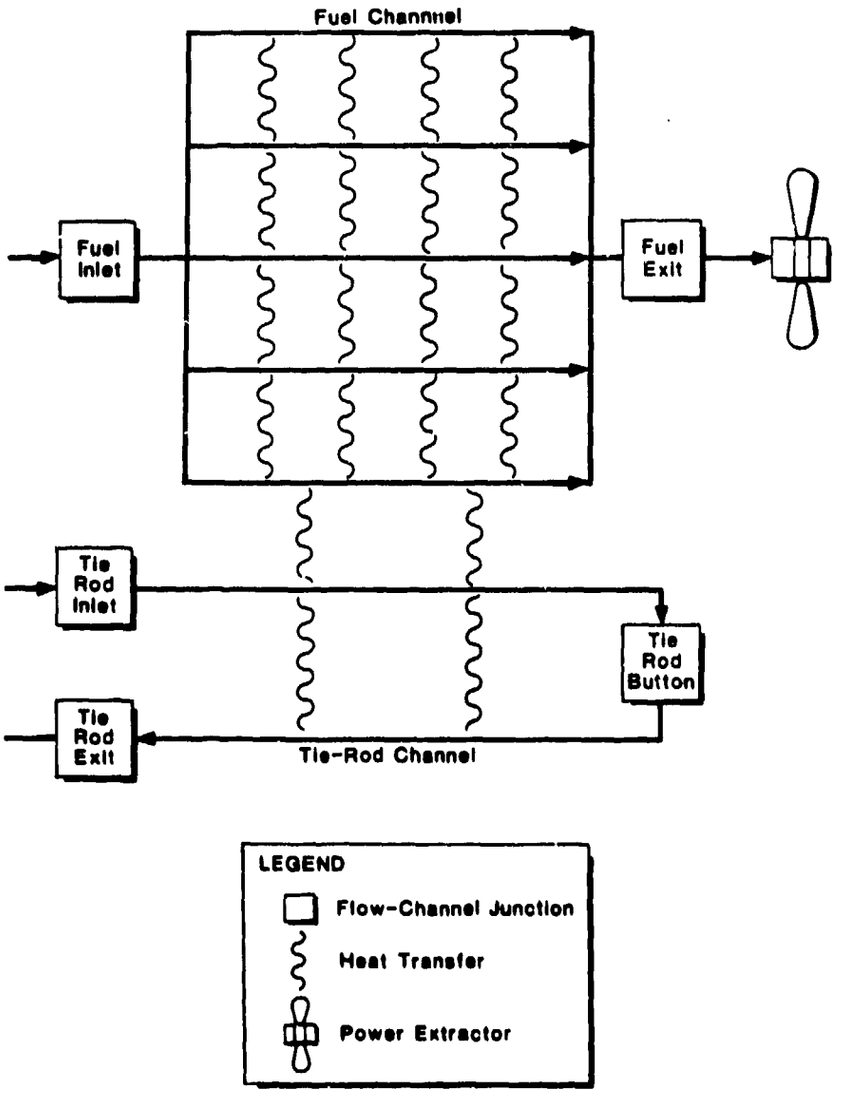

Fig. 10

CPTION flow diagram showing flow channels, flow junctions and transverse heat-transfer paths between channels for cluster configuration shown in Figs. 8 and 9.

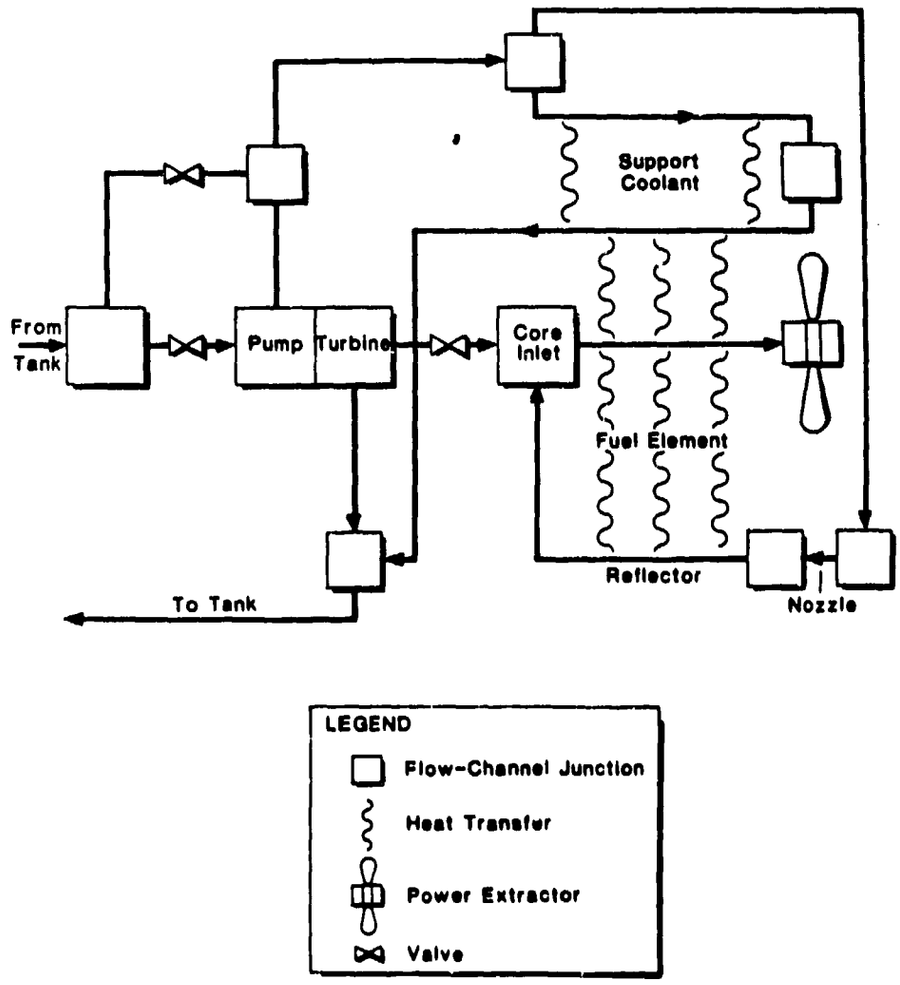

Fig. 11

OPTION flow diagram showing flow channels, flow junctions, valves, nozzle, reflector, pump, turbine, and transverse heat-transfer paths between channels for a complete space-power system as depicted in Fig. 5.

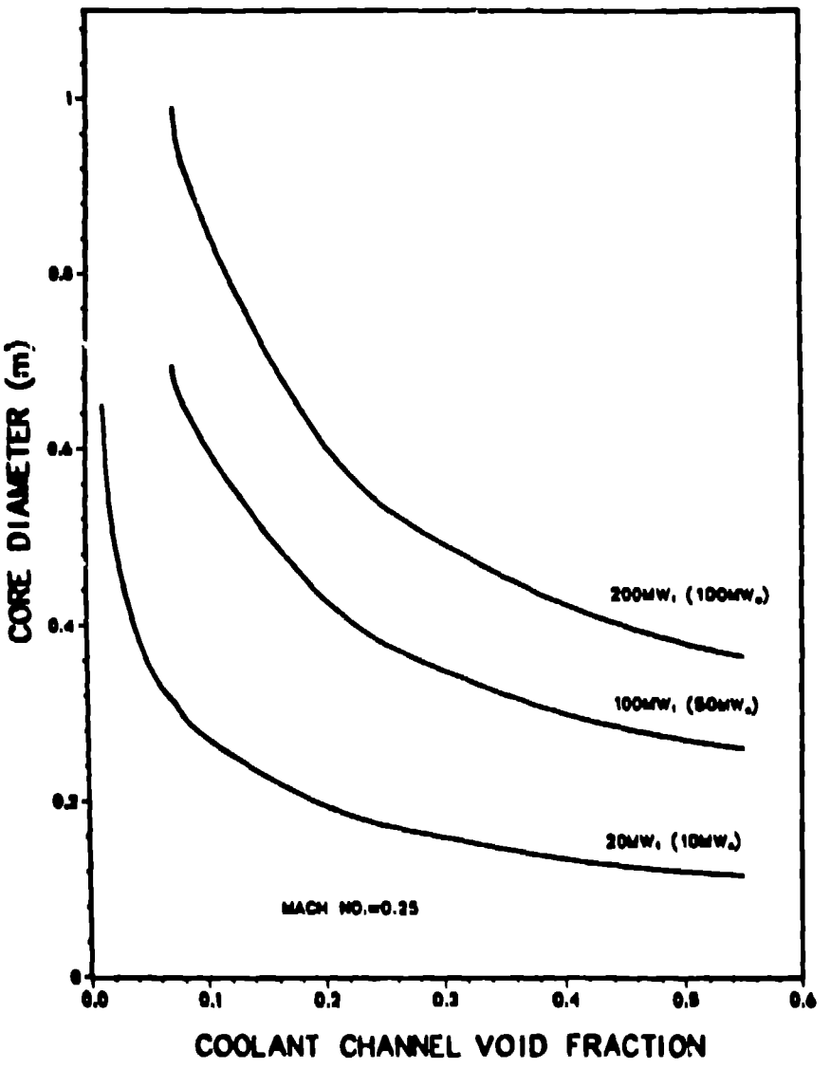

Fig. 12. Reactor core diameter (m) versus coolant channel void fraction for several power levels. MW_t is thermal power level and MW_e is electrical power level. (conversion efficiency is 0.50). The calculations are for an inlet temperature of 370 K (666 R) and exit conditions of 1500 K (2700 R), 3.10 MPa (450 psia) and Mach number of 0.25.

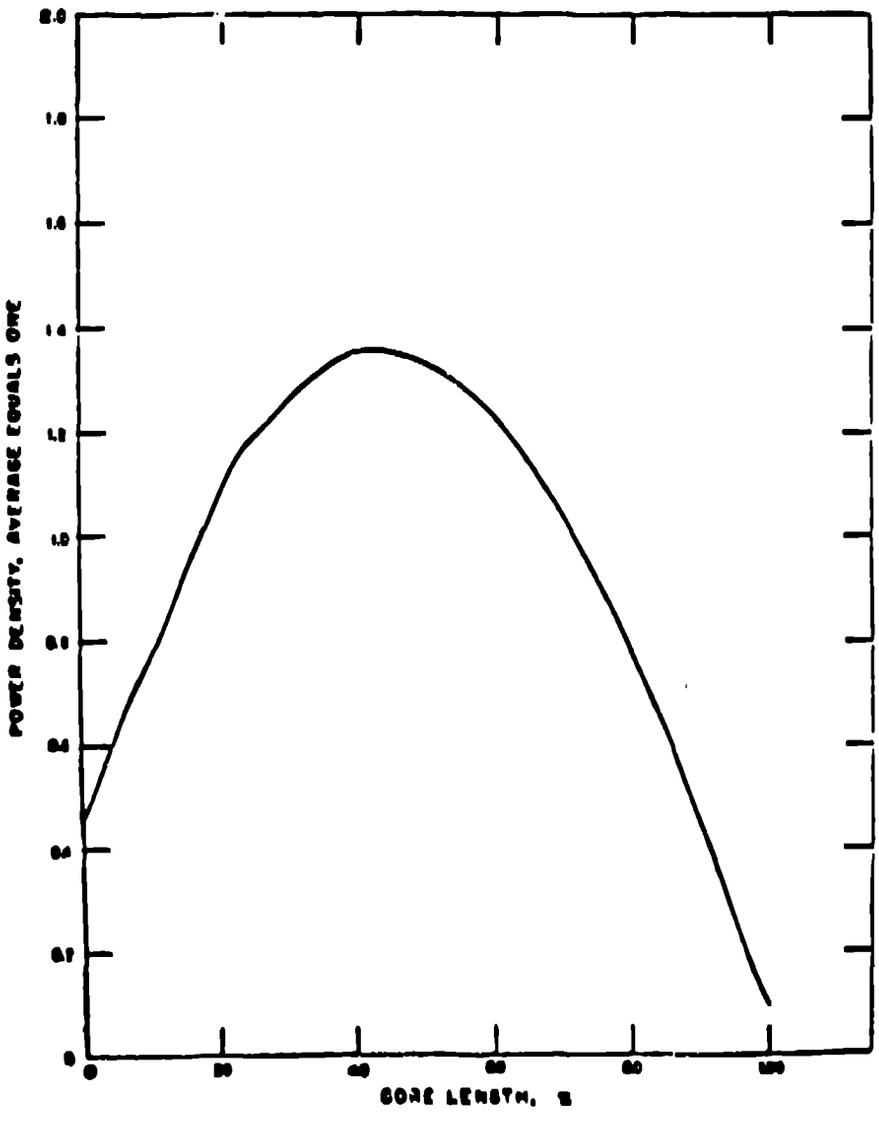

Fig. 13. Axial power profile used for OPTION thermal-fluid analysis.

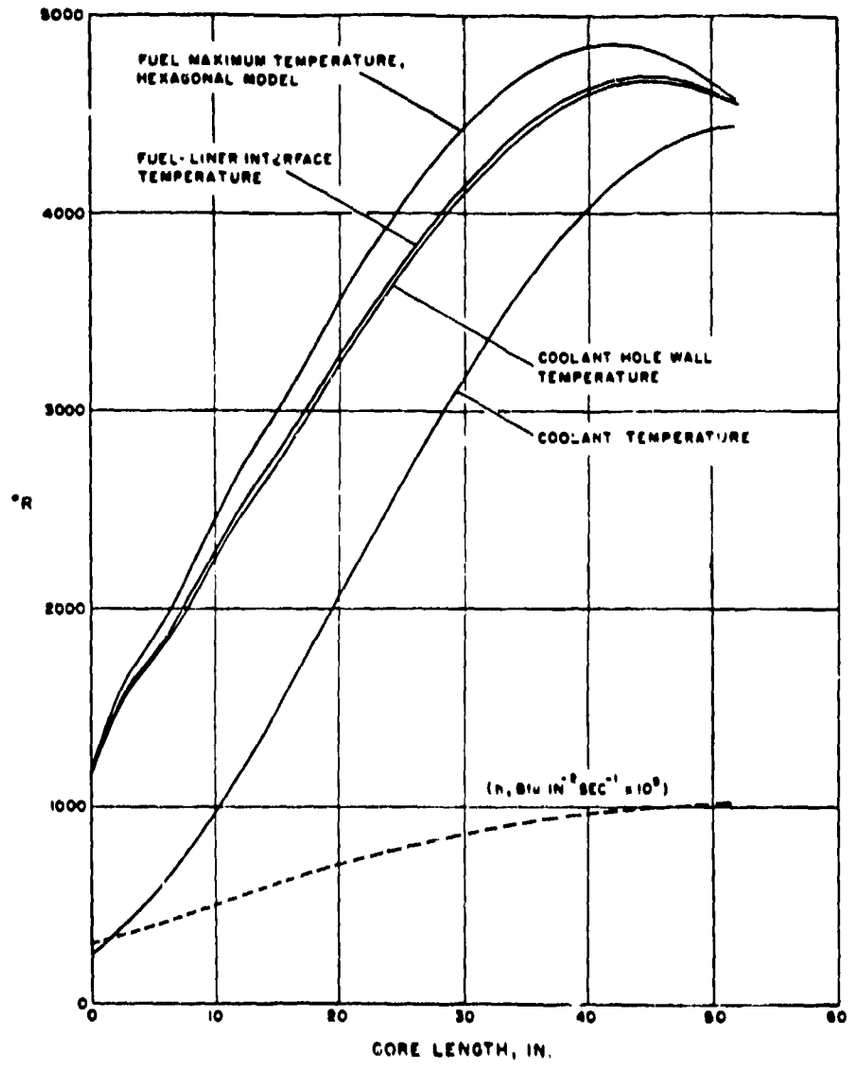

Fig. 14. Typical OPTION thermal-fluid code temperature and heat-transfer coefficient versus core length profiles.

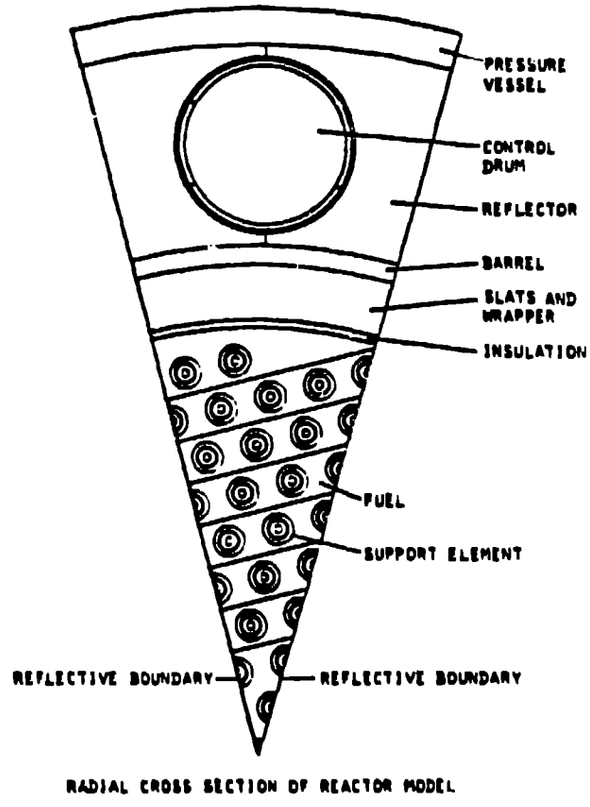

Fig. 15. Monte Carlo neutron and photon transport code radial cross section of reactor.

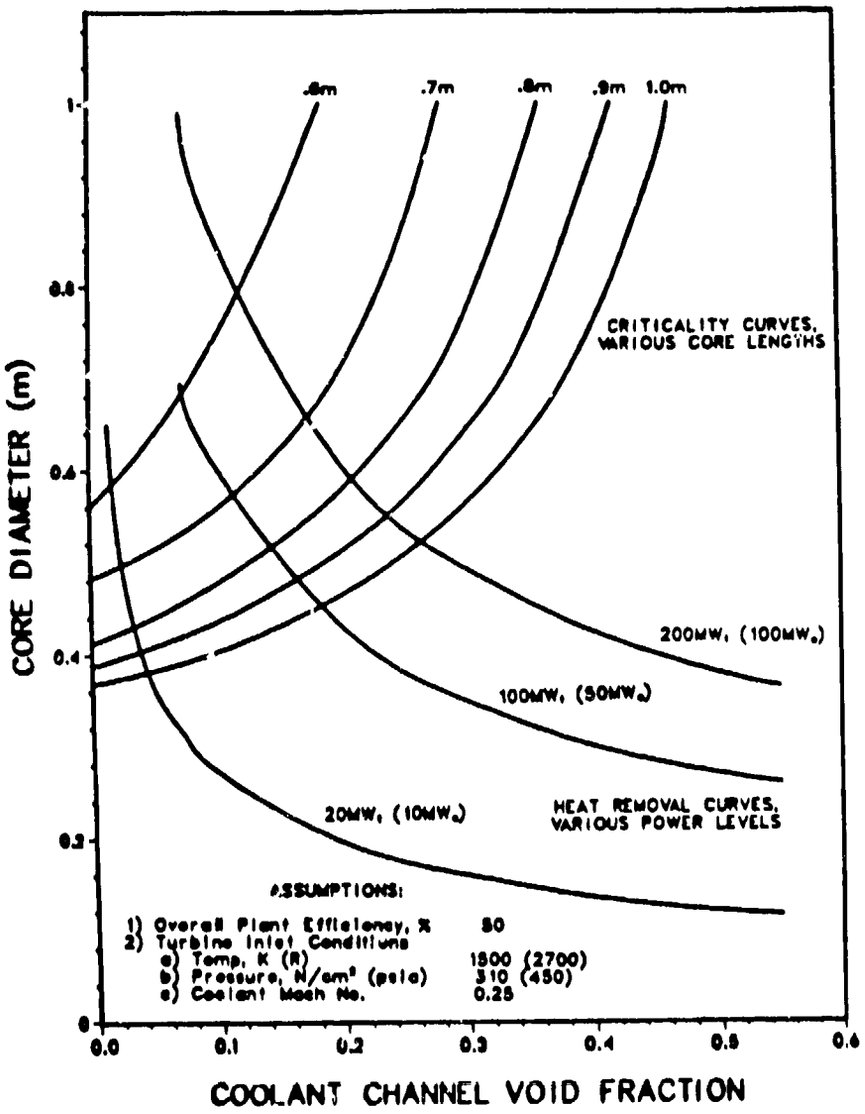

Fig. 16. Thermal-fluid and neutronic analysis results. A mass analysis at the intersections of these results is shown in Fig. 17.

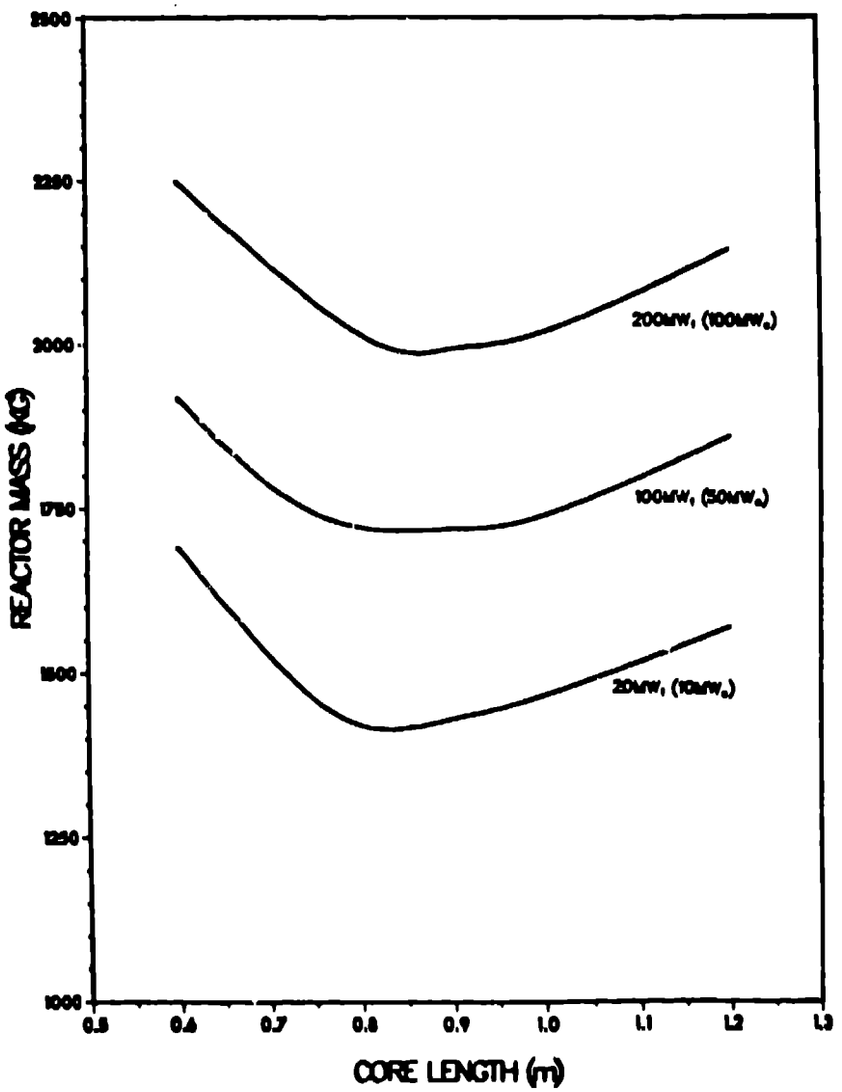

Fig. 17. Core length versus reactor mass for several power levels based on the thermal-fluid and neutronic analytical results given in Fig. 16.

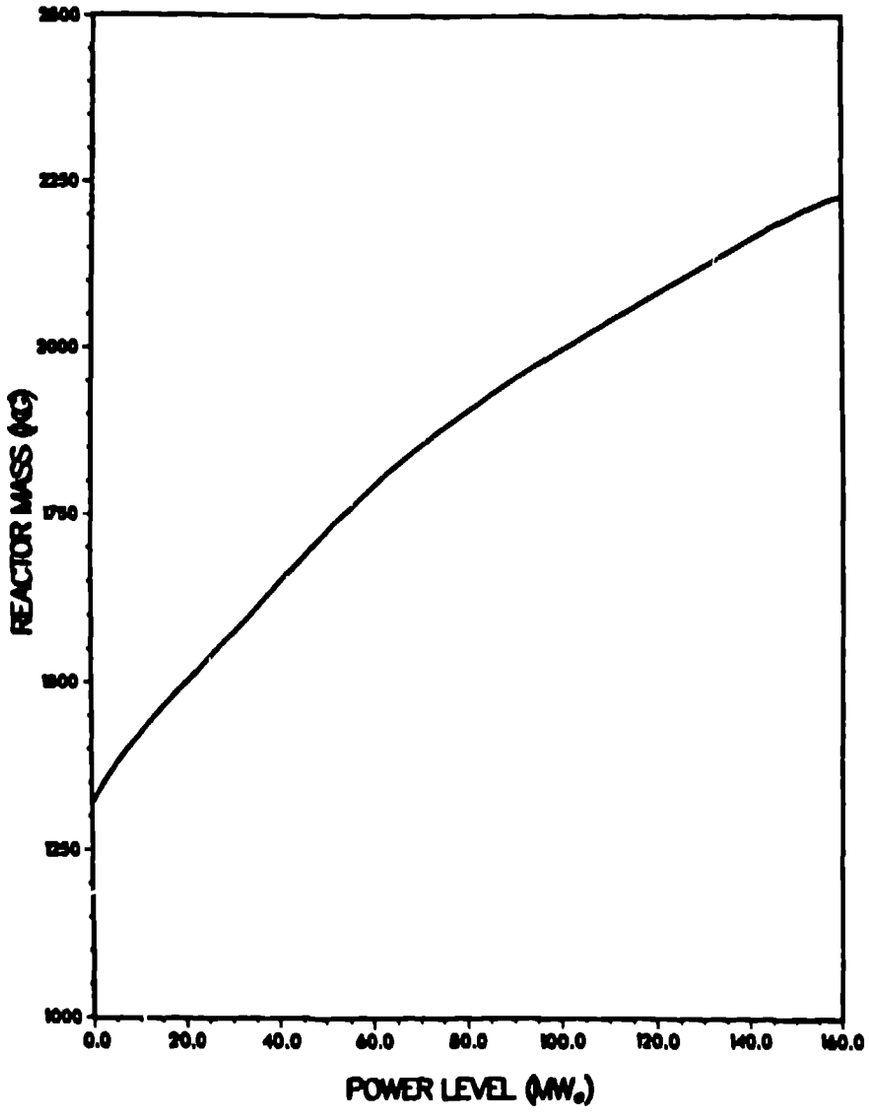

Fig. 18. Power level versus reactor mass corresponding to the minimum core diameters for the curves of Fig. 17.